

INSIGHTS INTO THE MECHANISM OF Cu^{2+} BINDING ONTO CHITOSAN-BASED CRYOGEL COMPOSITES: EQUILIBRIUM, KINETICS AND THERMODYNAMICS STUDIES

MARIA VALENTINA DINU, IONEL ADRIAN DINU, MARIA MARINELA LAZAR and ECATERINA STELA DRAGAN

“Petru Poni” Institute of Macromolecular Chemistry, Department of Functional Polymers, 41A, Grigore Ghica Voda Alley, Iasi 700487, Romania
 ✉ *Corresponding author: Maria Valentina Dinu, vdinu@icmpp.ro*

Received November 2, 2017

In this study, chitosan-based cryogel composites were prepared by combining the ion-imprinting methodology with ice-templating approach and were used as sorbents for Cu^{2+} ions. To understand the mechanism of Cu^{2+} sorption onto ion-imprinted cryogel composites (II-CCs), a systematic analysis of sorption isotherms, kinetics and thermodynamics data was performed. Accordingly, the Cu^{2+} sorption was a spontaneous endothermic monolayer sorption with chemisorption as the rate-limiting step. A faster sorption of Cu^{2+} ions was observed for II-CCs (20 min) compared to the non-imprinted ones (60 min), which was most probably caused by the presence of imprinted cavities. The reusability of II-CCs was also investigated and it was shown that the sorption capacity of II-CCs towards Cu^{2+} remained almost unchanged after five cycles of sorption/desorption.

Keywords: composites, copper ions, kinetics, sorption isotherms

INTRODUCTION

Heavy metal ion pollution is a worldwide problem that is mainly associated with areas of intensive industry. Among the heavy metal contaminants, copper is one of the most widely used metals, being released into the environment through various activities, including mining, metallurgy, fertilizer production, wood manufacturing and plumbing battery industries. Even though copper is an essential element in various processes of living systems, its presence in excessive amounts can irreversibly harm the body, causing headaches, stomachaches, kidney and liver damage (Wilson's disease), dizziness and diarrhea.^{1,2} The US Environmental Protection Agency (EPA) defines the Cu^{2+} permissible limit of 1.3 mg L^{-1} in drinking water,³ while the maximum acceptable concentration of Cu^{2+} in wastewaters disposed into the sewerage pipelines is 0.2 mg/dm^3 according to NTPA-002/2002 (Romanian Government).⁴ Consequently, the international and national requirements on the permissible limit/concentration of Cu^{2+} ions in the drinking water or wastewater led to the

development of numerous water treatment technologies. Several conventional approaches, including chemical precipitation, ion exchange, flocculation, electrochemical treatment, reverse osmosis, membrane filtration technologies and adsorption have been extensively implemented to remove Cu^{2+} ions from wastewaters.^{5,6} Among them, adsorption was proved to be a cost-effective technique, being especially utilized when the removal of Cu^{2+} ions from dilute aqueous systems is required.⁵⁻⁸

A variety of sorbents for Cu^{2+} removal has been extensively investigated in water treatment, including waste biomass,⁶ activated carbon,⁸ wheat straw lignin,⁹ agricultural by-products,¹⁰ as well as chitosan (CS) and its derivatives.¹¹⁻¹³ Among these materials, CS has been considered as an ideal candidate for Cu^{2+} sorption due to the presence of a multitude of $-\text{NH}_2$ and $-\text{OH}$ functional groups, which can serve as active sites to chelate/bind metal ions. However, the sorption performance of CS-based sorbents is controlled by the environment particularities (pH, ionic

strength, temperature) and biopolymer properties (degree of acetylation, molar mass, porosity).^{11,12} Therefore, CS-based composite sorbents endowed with enhanced Cu²⁺ sorption capacity and improved chemical and mechanical stability during regeneration and reusing cycles have been synthesized by embedding different compounds, such as clinoptilolite,¹⁴ Al₂O₃,¹⁵ Fe₃O₄,¹⁶ polyacrylamide-*co*-polyacrylate,¹⁷ poly(vinylamine),^{18,19} or potato starch-*graft*-polyamidoxime, within the CS matrix.²⁰ The development of highly selective sorbents for decontamination of wastewaters and recycling of residual metal ions requires a plenitude of recognition sites and tailored morphologies. Therefore, in this work, we investigate the Cu²⁺ binding onto novel ion-imprinted CS-based cryogel composite (II-CCs) sorbents that have permanent porosity and well-defined recognition sites. The formation of II-CCs sorbents based on CS, polyacrylamide and a natural zeolite, as monoliths, was achieved by combining the ion-imprinting methodology with unidirectional freezing (UF) approach. The sorption of Cu²⁺ ions onto II-CCs sorbents was examined compared to non-imprinted ones. The influence of sorbent dose, pH, initial Cu²⁺ concentration and contact time was studied in batch mode. Deeper insights into the mechanism of Cu²⁺ sorption onto CS-based cryogel composites were acquired from the systematical analysis of sorption isotherms, kinetics and thermodynamics data.

EXPERIMENTAL

Materials

Chitosan (CS) with a molar mass of 330 kDa and a degree of acetylation of 15%, glutaraldehyde (GA), acrylamide (AAm), N,N'-methylenebisacrylamide (BAAm), ammonium persulfate (APS) and N,N,N',N'-tetramethylethylenediamine (TEMED) were purchased from Sigma-Aldrich and used to prepare the composite sorbents. A natural zeolite coming from Macicás area (Cluj County, Romania), as particles with sizes ranging from 0.032 up to 0.050 mm, was selected to be embedded into the reactants mixture to control the water uptake of the final materials. Stock solutions of APS and TEMED were prepared by dissolving either 0.2 g of APS or 0.625 mL of TEMED in 25 mL of MilliQ water. Stock solutions of BAAm were prepared by dissolving the desired amount of BAAm, calculated for a certain monomer/cross-linker ratio, in 10 mL of MilliQ water, under stirring at 30 °C, and then stored for 24 h before use for composite synthesis. CuSO₄·5H₂O, (from Aldrich) was used as metal ion source for sorption experiments.

Synthesis and characteristics of composite sorbents

II-CCs were prepared by simultaneous *in situ* cross-linking of Cu²⁺/CS/zeolite mixtures by GA and polymerization of AAm in the presence of BAAm, using UF methodology. GA was used as cross-linker for CS, while BAAm as cross-linker for AAm. The BAAm/AAm molar ratio was 1:60, the weight ratio between CS and zeolite was 4:1, while 25 mg of CuSO₄·5H₂O were used for the pre-formation of Cu²⁺ recognition/imprinting sites. To illustrate the synthetic procedure, the details for preparation of the composite sorbents at initial concentrations of CS, AAm and GA of 2 wt%, 15 wt%, and 2.5 wt%, respectively, are presented below. In brief, 10 mL of 2 wt% acetic acid solution were added over the mixture of 25 mg of CuSO₄·5H₂O and 0.3 g of CS, to produce a dispersed phase. This mixture was rigorously stirred for 24 h in order to ensure the chelation of Cu²⁺ ions by functional groups of CS. After that, 74 mg of zeolite dispersed in 2 mL of MilliQ water were added over the Cu²⁺/CS mixture and kept under stirring for 1 h, followed by the dropwise addition of 0.64 mL of GA. The whole mixture was cooled down to 0 °C on an ice-bath and kept under stirring for 30 min. Simultaneously, 0.722 g of AAm was dissolved in 2 mL of MilliQ water and then stock solutions of BAAm (1 mL), and TEMED (1 mL) were added. The resulted mixture was also cooled down to 0 °C on an ice-water bath for 30 min. After that, the second mixture was added dropwise onto the CS/zeolite/GA mixture, under vigorous stirring. The dispersion containing CS, zeolite, GA, AAm, BAAm and TEMED, with the pH adjusted to 5.5 by adding 0.36 mL NaOH solution (0.5 M), was purged with nitrogen gas for 20 min. Finally, the APS stock solution (1 mL) was added over, and the whole mixture was further stirred for about 1 min. Aliquots from this mixture were transferred into 5 mL syringes, sealed with Parafilm, and then the bottom of the filled syringes was maintained close to the surface of liquid nitrogen (LN), -196 °C, used as freezing agent, in order to control the growth direction of ice crystals. After the complete freezing of the reaction mixture (about 7 min), the syringes were transferred into a CC1-K6 Huber Cryostat at -18 °C for 24 h. The syringes were taken out from the cryostat, maintained at RT for 1 h, and then the gels were carefully taken out, cut as discs of 3 mm height, and immersed in 100 mL ethylenediamine tetraacetic acid (EDTA -0.05 mol L⁻¹) to wash out the imprinted Cu²⁺ ions. The desorbed II-CCs were gradually washed with water/ethanol mixtures (50/50 for 1 h, and 80/20 for 2 h), and finally with MilliQ water for 72 h, until no Cu²⁺ ions were detected in the washing solution. Thereafter, the swollen II-CCs were frozen in LN and freeze-dried in a Martin Christ, ALPHA 1-2LD apparatus for 48 h, at -57 °C and 0.045 mbars. Non-imprinted CS-based cryogel composites (NI-CCs) were synthesized, purified and dried as described above for II-CCs and were used as controls. To further improve the overall

chelating performance of the composite cryogels, carboxylate groups were introduced by partial hydrolysis of amide moieties from PAAm. Thus, 0.5 g of dried II- or NI-CCs were added over 50 mL of 0.5 M NaOH solution, and kept under stirring for 7 h, and then intensively washed with MilliQ water up to neutral pH. Thereafter, all the composites were freeze-dried and stored under vacuum in the presence of P₂O₅, until a constant weight was reached. Some characteristics of the hydrolyzed CS-based composite sorbents used in this study for Cu²⁺ sorption are presented in Table 1.

Sorption studies

Cu²⁺ ion retention experiments of composite sorbents were carried out using a batch procedure on a water bath temperature-controlled shaker (GFL 1083, Gemini BV). To investigate the impact of sorbent dose on sorption capacity, various amounts of either II-CCs or NI-CCs, as discs (0.0025-0.02 g) were added into 10 mL of Cu²⁺ solution (200 mg L⁻¹). The influence of pH on the sorption capacity of both II- and NI-CCs was examined over a pH range of 3.0-6.0 at 298 K, using the same Cu²⁺ concentration. The initial solution pH was adjusted to the desired value with 1 M HCl or 1 M NaOH, and was not controlled afterwards. The influence of initial Cu²⁺ concentration was studied by equilibration of 0.01 g dried gel in 10 mL of Cu²⁺ aqueous solutions with concentrations ranging from 50 to 1000 mg L⁻¹. The vials containing the Cu²⁺ solution and the sorbent discs were placed on a water bath temperature-controlled shaker for 24 h. The Cu²⁺-loaded composites were separated from the solution by decantation and the concentration of the Cu²⁺ ions remaining in the filtrate was analyzed by UV-Vis spectroscopy at 808 nm (the maximum absorption

wavelength of CuSO₄·5H₂O),⁷ using a UV-Vis SPECORD200 Carl Zeiss Jena (Germany). The amount of Cu²⁺ sorbed at equilibrium on either II- or NI-CCs, in mg g⁻¹, was calculated by Eq. (1).²⁰

$$q_e = \frac{(C_o - C_e)V}{W_d} \quad (1)$$

Where C_o is the initial Cu²⁺ concentration, mg L⁻¹; C_e is the concentration of Cu²⁺ in aqueous solution at equilibrium, mg L⁻¹; V is the volume of aqueous solution, L, and W_d is the sorbent dose, g.

Eq. (2) was used to calculate the removal efficiency (RE , %) of Cu²⁺ ions from the aqueous solution:

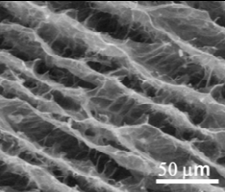
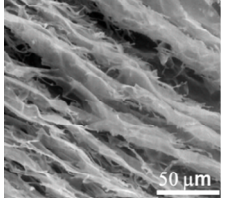
$$RE(\%) = \frac{C_o - C_e}{C_o} \times 100 \quad (2)$$

Where C_o and C_e have the same meaning as in Eq. (1). The average of three independent replicates was reported for each sorption experiment.

The kinetics experiments were performed only for the II-CCs because of their higher Cu²⁺ sorption capacity. The kinetics of Cu²⁺ removal was investigated at 298 K by immersing 0.01 g dried discs in 10 mL Cu²⁺ solutions with concentrations varying in the range of 50 to 444.5 mg L⁻¹. The Cu²⁺ concentration in aqueous solutions after sorption onto II-CCs was measured at fixed intervals of time between 5 min and 180 min.

The reusability of the composite sorbents was also evaluated. Thus, desorption studies were carried out in batch mode using 0.01 g of Cu²⁺-loaded composites, immediately after the sorption experiment. Herein, solutions of 0.1 M HCl were used as desorption media for all the experiments. The recovered composites were subsequently involved in five sorption/desorption successive cycles.

Table 1
Characteristics of CS-based cryogel composites used for Cu²⁺ sorption

Sample code ^a	Internal morphology	Pore sizes, ^b μm	Water uptake, ^c g g ⁻¹		
			pH = 2	pH = 4.5	pH = 8
II-CC15.H		38 ± 5 μm	24.66	31.5	37.1
NI-CC15.H		32 ± 3 μm	18.4	25.65	30.4

^aThe number "15" from the sample code indicates the initial concentration of AAm from the reaction mixture and the term "H" shows that the samples were hydrolyzed; ^bThe pore sizes were measured from three individual SEM micrographs with Image J 1.48v analyzing software; ^cWater uptake (WU) was gravimetrically evaluated and calculated as follows: $WU = (W_w - W_d)/W_d$, where W_w and W_d are the masses of wet and dry monoliths, respectively

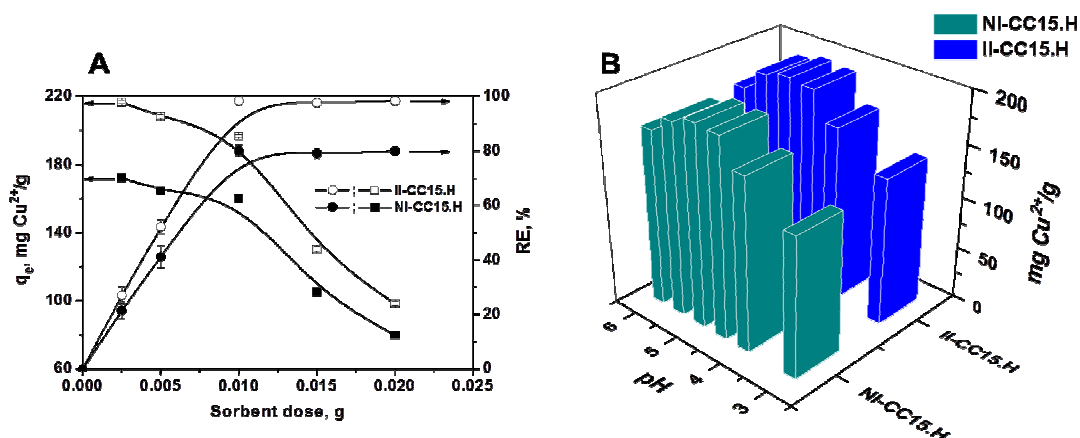


Figure 1: (A) Effect of sorbent dose on the sorption capacity of Cu²⁺ onto both NI- and II-CCs at initial pH and Cu²⁺ concentration values of 4.5 and 200 mg L⁻¹, respectively; (B) Influence of composite structure and solution pH on the sorption capacity of Cu²⁺ ions at a sorbent dose of 0.01 g and an initial Cu²⁺ concentration of 200 mg L⁻¹; (Parameters kept constant during sorption experiments: volume of solution = 0.01 L, contact time = 8 h, and temperature = 298 K)

To determine the thermodynamics parameters, the retention capacity of both II- and NI-CCs was studied at 298, 308 and 318 K, respectively.

Batch sorption processes are optimized and designed using isotherms and kinetics equations, and the aim of these optimization steps is to develop more efficient and simpler sorption processes. Two different error functions were used to determine the validity of both isotherms and kinetic models, which were fitted by the non-linear regression method: coefficient of determination (R^2), and the non-linear Chi-square (χ^2) test, mathematically estimated by Eq. (3):

$$\chi^2 = \sum \frac{(q_{e,exp} - q_{e,calc})^2}{q_{e,calc}} \quad (3)$$

RESULTS AND DISCUSSION

The CS-based cryogel composites, as monoliths, were prepared by *in situ* synchronous cross-linking of pre-formed Cu²⁺/CS complexes by GA and polymerization of AAm in the presence of BAAM, using UF methodology. The geometry of pre-organized Cu²⁺/NH₂ imprinted sites was preserved throughout the cross-linking of CS chains by GA, while the leaching step (Cu²⁺ removal by EDTA) generated well-defined 3D cavities, which form a favorable environment for selective rebinding of template ions. To further improve the overall chelating performance of the cryogel composites, carboxylate groups were introduced by partial hydrolysis of amide moieties from PAAM. The hydrolyzed cryogel composites exhibited a porous tube-like morphology (Table1, column 2) with an average of pore diameters of

about $38 \pm 5 \mu\text{m}$ for II-CC15.H and $32 \pm 3 \mu\text{m}$ for NI-CC15.H.

To select the optimum Cu²⁺sorption conditions for these cryogel composites, the influence of sorbent dosage and pH solution, two parameters with a significant impact on metal ion sorption, was first investigated (Fig. 1).

An expected increase of Cu²⁺ removal occurred for all the composites with the increase of sorbent dose, with a sharp increase up to about 100% for II-CCs, and nearly 80% for NI-CCs, when the sorbent dosage rose from 0.0025 up to 0.01 g (Fig. 1A). This common increment in removal efficiency is attributed to the increasing number of sorbent sites available for Cu²⁺ sorption, while the number of Cu²⁺ ions in contact with the sorbent weight unit decreased, leading to an unsaturation of sorption sites.²¹ To further evaluate the effect of sorbent structure on its sorption properties, the optimal sorbent dose of 0.01 g was chosen for all upcoming sorption experiments.

The pH of the aqueous solution also has a strong effect on the sorption process because both the metal ion speciation and the surface charge of the sorbent are highly dependent on the pH value.^{11,21,22} Cu²⁺ commonly precipitates in the form of metal oxides or hydroxides at pH > 5.5, while the pH variation induces changes in the total charge of composites, due to the presence of ionizable groups (NH₂ and COOH). Therefore, the influence of pH on the amount of Cu²⁺ ion sorbed at equilibrium by both the II- and NI-CCs

was investigated in aqueous solutions with initial pH values ranging from 3 to 6, while all the other parameters affecting the sorption process were kept constant.

Figure 1B clearly shows the dependence of sorption capacity on pH, the Cu^{2+} sorption increasing with the increase of pH in the range of 3 to 5, at which a maximum amount of Cu^{2+} ions was retained onto the composites. This tendency indicates a decreasing number of protonated amine groups, leading to a less positively charged cryogel structure, and demonstrating the rising amount of binding sites available for chelating Cu^{2+} ions. A similar pH influence has been previously reported for sorption of Cu^{2+} on other sorbents.^{21,23} However, a further increase of pH up to 6 resulted in a decrease of Cu^{2+} sorption, which was probably caused by a phase separation of Cu^{2+} as hydroxides. To better understand this trend, the pH corresponding to the deposition of $\text{Cu}(\text{OH})_2$ was calculated as previously described,⁷ the resulting pH being about 5.4 for an initial Cu^{2+} concentration of $0.0031 \text{ mol L}^{-1}$. Consequently, the precipitation of $\text{Cu}(\text{OH})_2$ started at pH values higher than 5.4, leading to an apparent decrease of sorption capacity. In this context, the initial pH of the Cu^{2+} solutions was kept constant at 4.5 for the kinetics and equilibrium measurements. In general, the II-CCs exhibited higher sorption capacities when compared with the corresponding

NI-CCs, regardless the pH value (Fig. 1B). The enhanced retention of Cu^{2+} ions by imprinted cryogels, compared to the non-imprinted ones, proves that the sorption is not only caused by the binding ability of amine groups, but also by their controlled spatial organization into Cu^{2+} -imprinted cavities during cryogelation.

Sorption isotherms

The maximum amount of metal ions that are retained onto sorbents is generally evaluated from sorption isotherms. The experimental isotherms for sorption of Cu^{2+} ions from synthetic wastewaters onto II-CC15.H and NI-CC15.H are depicted in Figure 2.

The isotherms have a typical “H” shape, indicating a high affinity of our composites for Cu^{2+} ions.^{20,24,25} Fitting the equilibrium data with various isotherm models is commonly performed to establish the most appropriate theoretical model able to describe the sorption of ionic species onto sorbents.^{26,27} The Cu^{2+} sorption data were fitted with five isotherm models, including Langmuir, Freundlich, Temkin, Dubinin–Radushkevich (D–R), and Sips (Fig. 2), using the non-linear regression method.^{26,28} The values of model isotherm parameters, coefficients of determination (R^2), and non-linear Chi-square test (χ^2) are presented in Table 2.

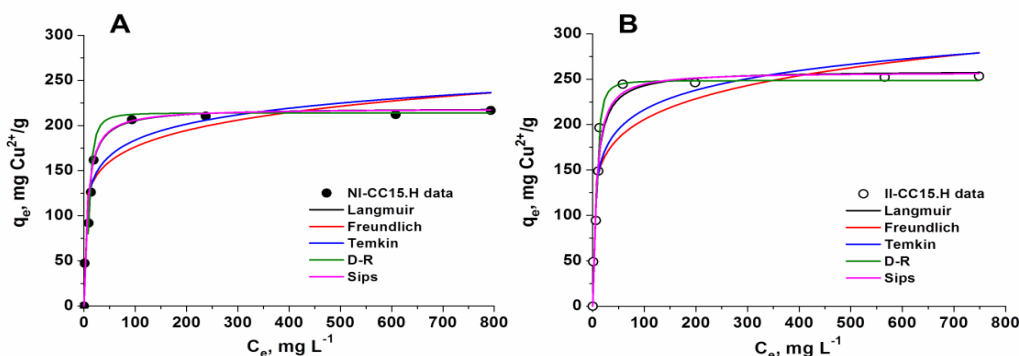


Figure 2: Equilibrium sorption of Cu^{2+} ions onto NI-CC15.H (A) and II-CC15.H (B) fitted with five non-linear isotherm models

The high values of R^2 and the low values of χ^2 obtained with the Langmuir isotherm support this model as the best theoretical approach for describing the equilibrium sorption data of Cu^{2+} ions onto both NI-CC15.H and II-CC15.H. These findings suggest the monolayer coverage of Cu^{2+} ions onto the homogeneous surface of the sorbents.

The dimensionless constant R_L (Eq. (4)), also known as the constant separation factor or equilibrium parameter, was used to assess the feasibility of sorption in a certain concentration range:²⁹

$$R_L = \frac{1}{1 + K_L C_i} \quad (4)$$

where K_L is the Langmuir sorption constant ($L\ mg^{-1}$), and C_i is the initial concentration of Cu^{2+} ions ($mg\ L^{-1}$). Accordingly, the sorption is unfavorable when $R_L > 1$, linear when $R_L = 1$, favorable when $0 < R_L < 1$, and irreversible when $R_L = 0$.^{20,29} The R_L values for the Cu^{2+} sorption under non-competitive conditions onto NI- and II-

CCs, calculated with Eq. (4) at various initial Cu^{2+} concentrations (50-1000 $mg\ L^{-1}$) range from 0.064 to 0.0068 for NI-CC15.H, and from 0.615 to 0.074 for II-CC15.H, indicating a favorable sorption of Cu^{2+} at equilibrium for both composite sorbents.

Table 2
Equations of model isotherms and the values of corresponding parameters obtained using the non-linear regression method for sorption of Cu^{2+} ions onto both NI- and II-CCs, at 298 K

Isotherm	Equation	Parameters	Sorbent	
			NI-CC15.H	II-CC15.H
Langmuir	$q_e = \frac{q_m K_L C_e}{1 + K_L C_e}$	$q_m, mg\ g^{-1}$	219.59	259.56
		$K_L, L\ mg^{-1}$	0.15	0.01
		R^2	0.958	0.967
		χ^2	317.32	309.88
		$K_F, mg\ g^{-1}$	92.22	102.24
Freundlich	$q_e = K_F C_e^n$	$1/n$	0.14	0.15
		R^2	0.828	0.839
		χ^2	1143.77	1509.66
		$b_T, J\ mol^{-1}$	97.38	79.84
Temkin	$q_e = \frac{RT}{b_T} \ln a_T C_e$	$a_T, L\ mg^{-1}$	13.80	10.68
		R^2	0.814	0.819
		χ^2	788.98	943.33
		$q_{DR}, mg\ g^{-1}$	214.08	248.51
D-R	$q_e = [q_{DR} \exp\{-\beta [RT \ln(1 + \frac{1}{C_e})]\]^2\}$	$\beta, mol^2\ kJ^{-2}$	1.6510 ⁻⁴	1.110 ⁻⁴
		$E, kJ\ mol^{-1}$	55.25	67.57
		R^2	0.945	0.954
		χ^2	362.93	437.16
		$q_m, mg\ g^{-1}$	218.88	257.47
Sips	$q_e = \frac{q_m a_S C_e^n}{1 + a_S C_e^n}$	a_S	0.13	0.12
		$1/n$	1.04	1.10
		R^2	0.945	0.962
		χ^2	369.26	356.34

q_m – maximum theoretical sorption capacity; K_L – Langmuir constant; K_F – Freundlich constant; n – a measure of the nature and strength of the adsorption process, and of the distribution of active sites related to the surface heterogeneity; the larger is its value, the more heterogeneous is the sorbent system; b_T – Temkin constant; a_T – equilibrium binding constant corresponding to the maximum binding energy; q_{DR} – maximum sorption capacity of metal ion; β – D-R isotherm constant; a_S – Sips constant; $1/n$ – values close to zero indicate a heterogeneous sorbent, while values closer to 1 indicate a relatively homogeneous distribution of binding sites; $1/n = 1$, Sips isotherm coincides with Langmuir equation

The Freundlich isotherm is an empirical equation used to model the sorption process onto heterogeneous surfaces, assuming the non-equivalence of binding sites. Even though the $1/n$ values lower than 1 support the feasibility of sorption for both composite cryogels, the low values of R^2 (< 0.84) and the high values of χ^2 (> 1140) demonstrate the poor applicability of the Freundlich isotherm for describing the experimental data. Analysis of fitting parameters obtained by applying the Temkin isotherm

showed that this theoretical model also fails to describe the sorption of Cu^{2+} ions onto these sorbents. This isotherm takes into account the interactions between sorbent and sorbate, and considers a linear decrease of sorption heat with the surface coverage, whereas the sorption process is characterized by the uniform distribution of bonding energies.^{27,30} The values of Temkin sorption potential, a_T , were 13.80 and 10.68 $L\ mg^{-1}$ for NI- and II-CCs, respectively, indicating a high potential of both composites for

sorption of Cu^{2+} ions. The low values of the Temkin constant, b_T , related to the heat of Cu^{2+} sorption of about 97.38 and 79.83 J mol^{-1} for NI-CC15.H and II-CC15.H, respectively, support a weak interaction between the Cu^{2+} ions and sorbent. However, the low R^2 values (< 0.8) and the high χ^2 values for both composites indicate that the Temkin model is not suitable to describe the sorption mechanism of Cu^{2+} ions.

In order to make a clear difference between the physical and chemical sorption of Cu^{2+} ions onto the composites, the D–R isotherm was applied. The mean free energy of sorption, E (kJ mol^{-1}), defined as the free energy of one mole of ions that is transferred from the infinity of solution to the surface of a solid, calculated with Eq. (5), is typically used to estimate the sorption type:²⁰

$$E = \frac{1}{(2\beta)^{1/2}} \quad (5)$$

Where β is the D–R isotherm constant. Values of E lower than 8 kJ mol^{-1} depict a physical sorption, while E values ranging from 8 to 16 kJ mol^{-1} characterize a sorption process occurring by an ion exchange mechanism. E values higher than 40 kJ mol^{-1} indicate chemisorption as the mechanism of sorption.^{22,27} The E values of 55.25 kJ mol^{-1} for NI-CC15.H and 67.57 kJ mol^{-1} for II-CC15.H

reveal the chemisorption as the main mechanism of Cu^{2+} sorption onto these composites. The q_{DR} values were in the same range as the values of q_m obtained by fitting the Langmuir isotherm (Table 2), which supports the applicability of the D–R isotherm in describing the sorption process. Subsequently, the compatibility of the Sips isotherm model for both composites, sustained by the high values of R^2 and the low values of χ^2 , as well as the calculated values of q_m , which were very close to the experimental ones, points out the homogeneous distribution of chelating sites onto the sorbent surface.

Kinetics

To properly design our sorbents, we also investigated the Cu^{2+} sorption and desorption kinetics, which offers further information on the rate of metal ion sorption or desorption, as well as a deeper insight into the sorption mechanism, by correlating the experimental data with several kinetic models. Herein, the sorption and desorption capacities of Cu^{2+} ions as a function of time for the hydrolyzed Cu^{2+} -imprinted composite cryogel, II-CC15.H, were evaluated over five reusing cycles, as shown in Figure 3.

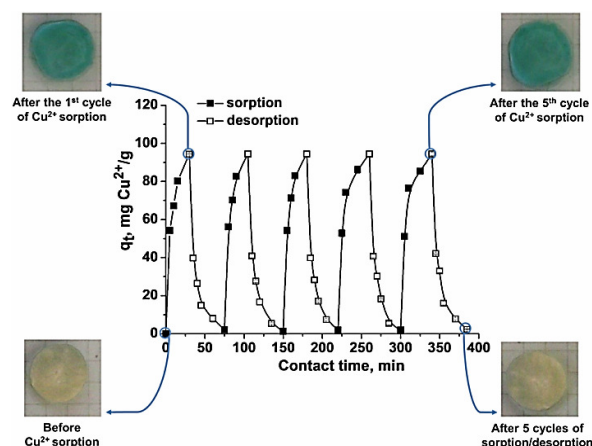


Figure 3: Sorption and desorption kinetics of Cu^{2+} ions onto/from II-CC15.H sorbent. Parameters kept constant during sorption kinetics include the initial Cu^{2+} concentration of 100 mg L^{-1} , sorbent dose of 0.01 g, and pH of 4.5. Cu^{2+} desorption was achieved by treatment with 0.1 N HCl solution. The optical images display the color difference between the cryo-composites as discs both before Cu^{2+} sorption and after the 5th cycle of elution (bottom images, yellowish discs), and after the 1st and 5th cycles of Cu^{2+} sorption (top images, blue discs)

A fast sorption of metal ions from synthetic wastewaters containing about 100 $\text{mg Cu}^{2+} \text{L}^{-1}$ was observed (Fig. 3), the sorption equilibrium being reached after 20 min. The rapid sorption

process was most probably induced by the combined effect of Cu^{2+} complexation rate, the presence of recognition sites within the II-CC structure, and its oriented, highly porous

morphology. Consequently, the desorption process was also very fast, the complete elution of Cu^{2+} ions being achieved in about 30 min (Fig. 3). The regeneration of sorbents and the recovery of metal ions in a concentrated form are key factors in the development of low-cost materials.^{7,20} In this respect, the composites were further involved in successive sorption/desorption cycles, after the adequate regeneration with 0.1 M NaOH. The almost constant sorption capacity of Cu^{2+} ions at equilibrium after five sorption/desorption cycles, as well as the unaffected disc shape of the composite, without cracks and defects, reveal the remarkable chemical and mechanical stability of II-CC15.H during the successive loading/leaching steps, as shown in Figure 3.

To investigate the sorption mechanism and the potential rate controlling steps, such as the mass transport and/or chemical reactions, a series of contact time experiments for Cu^{2+} ions retention onto NI- and II-CCs were carried out using initial Cu^{2+} concentrations ranging from 50 to 444.5 mg L^{-1} . A two-stage sorption behavior was observed for both types of composites, irrespective of the initial Cu^{2+} concentration (Fig. 4).

The II-CC15.H sorbents showed a faster sorption rate and a shorter equilibrium time for Cu^{2+} ions, compared to NI-CC15.H sorbents. For example, a fast uptake of Cu^{2+} ions occurred within the first 10 min at an initial Cu^{2+} concentration of 100 mg L^{-1} , reaching equilibrium in about 20 min when II-CC15.H was used as sorbent, while the sorption equilibrium was reached in about 60 min in the case of the NI-CC15.H sorbent. The faster kinetics of the II-CC15.H sorbents was apparently caused by the higher affinity of imprinted cavities of II-CC.H towards copper.

To get insights into the sorption mechanism, the kinetics data of Cu^{2+} sorption onto NI- and II-CCs were analyzed by applying the pseudo-first-order (PFO), pseudo-second-order (PSO) and intraparticle diffusion (IPD) kinetic models in the case of four initial Cu^{2+} concentrations, *i.e.* 50 mg L^{-1} , 100 mg L^{-1} , 200 mg L^{-1} and 444.5 mg L^{-1} respectively, (Fig. 4 and Table 3). The PFO kinetic model, also known as the Lagergren rate equation, considers the sorption rate proportional with the difference between the equilibrium sorption capacity and the sorbed amount.³¹ The PSO kinetic model assumes that the rate-limiting step is chemisorption, involving valence forces through sharing or exchanging electrons between the sorbent and sorbate.³²

Analysis of kinetics data demonstrates that the PSO kinetic model was the most accurate theoretical model and consistent with the experimental data, as shown by the higher R^2 and lower χ^2 values (Table 3). This conclusion underlines the dependence of Cu^{2+} sorption rate on the availability of sorption sites and emphasizes the chemical sorption as the rate-limiting step.^{20,21,33}

Typically, the sorption of molecules onto a sorbent involves several steps, two of them being the most important in an aqueous medium under stirring: (i) the transport of metal ions through the boundary layer from the sorbent surface, and (ii) the transport of solute from the sorbent surface into the pores.³⁰

The IPD model proposed by Weber and Morris is generally preferred to explain the diffusion mechanism of the sorption process.³⁴ The term C of the IPD model (Table 3) describes the effect of boundary layer thickness; therefore, a higher C value results in a greater contribution of the diffusion through the boundary layer onto the rate limiting step. When the linear plot of q_t versus $t^{0.5}$ passes through the axis origin, the sorption process is controlled only by the IPD.³⁰ In the case of multi-linear plots, each step may influence the sorption process.^{30,35} In this context, the IPD model was applied to the kinetics data obtained for Cu^{2+} sorption onto NI-CC15.H and II-CC15.H. The first region of the q_t versus $t^{0.5}$ plots (Figs. 4E and 4F) reveals the dominant effect of IPD onto the Cu^{2+} sorption and outlines the external resistance of this layer towards the Cu^{2+} mass transfer. The values of k_{id} , C and R^2 corresponding to this region are listed in Table 3. The slight increase of k_{id} values with the increase of initial Cu^{2+} concentration indicates a faster diffusion and sorption in this sorption step.³⁶ In the second region, the influence of IPD decreases considerably, due to the decrease of both the Cu^{2+} concentration in the aqueous phase and the number of active sites available for sorption. To this end, the rate controlling step in Cu^{2+} sorption onto NI- and II-CCs was controlled by a combination of factors, and not only by the IPD.

Thermodynamics

In environmental applications, both energy and entropy contributions must be considered in order to determine which process will spontaneously occur.³⁷ The thermodynamics parameters, such as free energy of sorption (ΔG°), enthalpy (ΔH°) and

entropy change (ΔS°), were evaluated by the Van't Hoff equation (Eq. (6)).

The equation correlates ΔH° and ΔS° with either the Langmuir constant, K_L ,^{22,25} or the distribution coefficient, K_D , (Eq. (7)):^{20,22}

$$\ln K_D = \frac{\Delta S^\circ}{R} - \frac{\Delta H^\circ}{RT} \quad (6)$$

where R (8.314 J mol⁻¹ K⁻¹) is the ideal gas constant;

$$K_D = \frac{q_e}{C_e} \quad (7)$$

where q_e is the sorption capacity, mg g⁻¹; C_e

represents the equilibrium concentration, mg L⁻¹.

The slope, $\Delta H^\circ/R$, and the intercept, $\Delta S^\circ/R$, obtained by plotting $\ln K_D$ versus $1/T$ (Fig. 5),

according to Eq. (6), led to the ΔH° and ΔS° values for Cu²⁺ sorption onto the composites, while the ΔG° values were calculated by Eq. (8) (Table 4):

$$\Delta G^\circ = -RT \ln K_D \quad (8)$$

The negative values of ΔG° for all the composites illustrate a spontaneous and thermodynamically favorable sorption. The decrease of the ΔG° value with the increase of temperature suggests an increasing degree of spontaneity during Cu²⁺ sorption. The sorption process is endothermic ($\Delta H^\circ > 0$), while the positive values of ΔS° demonstrate both the affinity of the sorbents for Cu²⁺ ions and the irregular increase of randomness at the composite-solution interface during sorption.

Table 3
Equations of applied kinetics models and the corresponding values of parameters obtained by non-linear regression method for sorption of Cu²⁺ ions onto II-CC15.H, at 298 K

Kinetic model	Parameters	NI-CC15.H				II-CC15.H			
		C_i , mg L ⁻¹				C_i , mg L ⁻¹			
		50	100	200	444.5	50	100	200	444.5
PFO, $q_t = q_e(1 - \exp^{-k_1 t})$	$q_{e,exp}$, mg g ⁻¹	46.57	90.01	161.24	210.53	47.46	94.46	196.60	246.90
	$q_{e,calc}$, mg g ⁻¹	40.89	83.00	195.30	258.02	44.32	100.09	223.72	280.12
	k_1 , min ⁻¹	0.10	0.04	0.04	0.03	0.26	0.14	0.05	0.05
	R^2	0.93	0.94	0.97	0.99	0.969	0.989	0.987	0.980
	χ^2	14.84	48.98	49.20	56.15	6.05	10.58	60.84	143.56
PSO, $q_t = \frac{q_e^2 k_2 t}{1 + q_e k_2 t}$	$q_{e,calc}$, mg g ⁻¹	45.40	96.42	161.43	208.64	46.28	94.21	195.79	242.13
	$k_2 \times 10^4$, g mg ⁻¹ min ⁻¹	30	5.31	1.92	1.09	113	24	3.06	2.04
	R^2	0.98	0.98	0.99	0.99	0.991	0.991	0.989	0.993
	χ^2	4.89	18.27	16.00	29.48	1.702	8.57	51.98	49.65
	C , mg g ⁻¹	15.62	10.34	-6.86	-10.23	25.19	28.09	11.43	16.36
IPD, $q_e = k_{id} t^{0.5} + C$	k_{id} , g mg ⁻¹ min ^{-0.5}	3.19	7.86	18.51	21.79	4.08	12.45	23.90	26.99
	R^2	0.89	0.99	0.93	0.97	0.682	0.963	0.984	0.989
	χ^2	3.86	5.53	84.46	27.28	4.98	4.41	35.72	6.02

q_e and q_t are the amount of Cu²⁺ ions sorbed at equilibrium and at time t , respectively; k_1 is the rate constant of PFO kinetic model; k_2 is the rate constant of PSO kinetic model; k_{id} is the intraparticle diffusion rate constant, and C is a constant describing the effect of boundary layer thickness

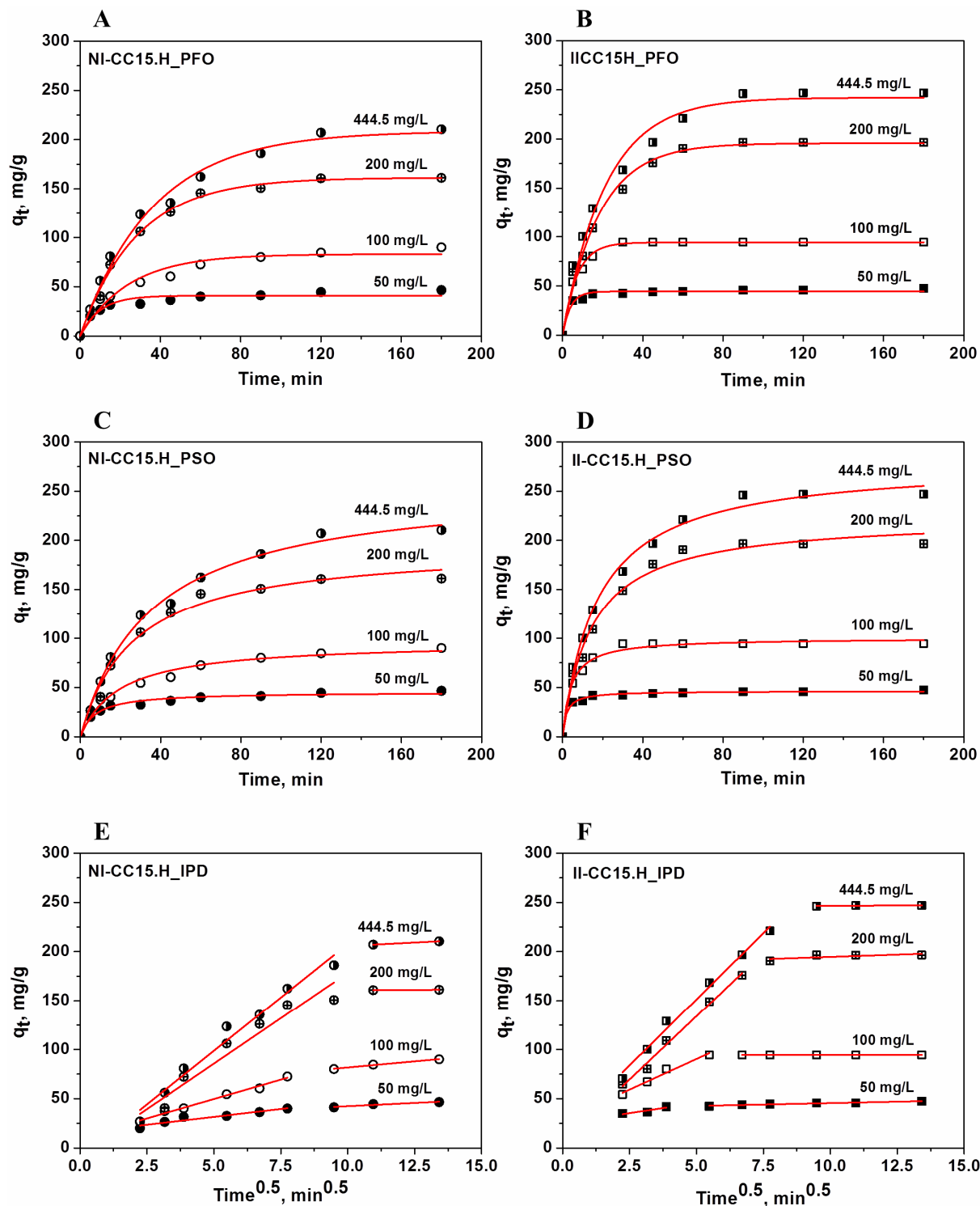


Figure 4: Sorption kinetics of Cu^{2+} onto NI-CC15.H and II-CC15.H sorbents fitted with PFO (A and B), PSO (C and D), and IPD (E and F) models at various initial Cu^{2+} concentrations, using wastewater solutions with a volume of 0.01 L and initial pH of 4.5, at constant sorbent dose of 0.01 g, and temperature of 298 K

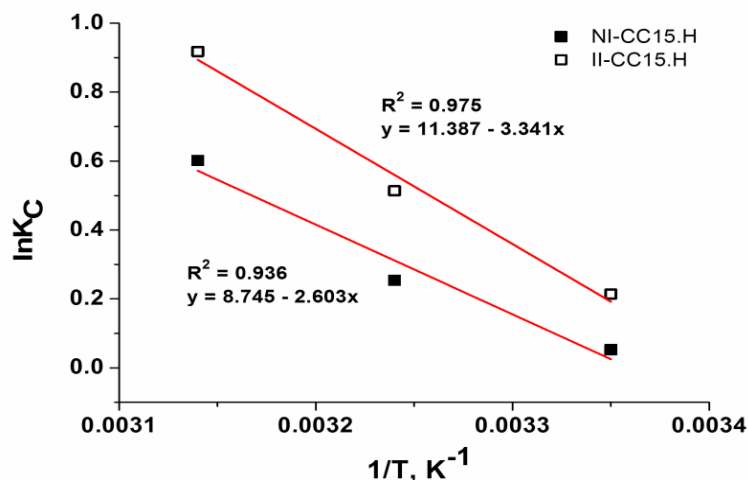


Figure 5: $\ln K_c$ versus $1/T$ for Cu^{2+} sorption onto NI- and II-CC sorbents

Table 4
Thermodynamics parameters of Cu^{2+} sorption onto NI- and II-CC15.H sorbents

Sample code	T , K	Thermodynamics parameters		
		ΔH° kJ mol ⁻¹	ΔS° J mol ⁻¹ K ⁻¹	ΔG° kJ mol ⁻¹
NI-CC15.H	298	21.643	72.81	-0.130
	308			-0.65
	318			-1.591
II-CC15.H	298	27.787	94.677	-0.53
	308			-1.316
	318			-2.427

CONCLUSION

Novel copper-imprinted CS-based cryogel composites, with an excellent Cu^{2+} binding capacity, and fast sorption rate have been reported in this study. Langmuir model was shown to better describe the sorption isotherms, with a maximum sorption capacity of 259.56 mg g⁻¹ for II-CC15.H and 219.59 mg g⁻¹ for NI-CC15.H. The kinetics data were well-fitted by the PSO kinetic model, supporting chemisorption as the rate-determining step of Cu^{2+} sorption. Moreover, the II-CC15.H sorbents have retained their capability to bind and recover Cu^{2+} ions during five reusing cycles without shape changes or decline of their sorption capacity. These results sustain the high potential of our composite sorbents in water remediation applications.

ACKNOWLEDGMENT: This work was financially supported by the project PN-II-ID-PCE-2011-3-0300.

REFERENCES

- ¹ H. Hu, in "Life Support: The Environment and Human Health", edited by M. McCally, Cambridge MIT Press, 2002, pp. 1-12.
- ² D. L. de Romana, M. Olivares, R. Uauy and M. Araya, *J. Trace Elem. Med. Bio.*, **25**, 3 (2011).
- ³ D. J. Fitzgerald, *Am. J. Clin. Nutr.*, **67**, 1098 (1998).
- ⁴ NTPA, Romanian Government, <http://legislatie.just.ro/Public/DetaliuDocument/34653>.
- ⁵ F. Fu and Q. Wang, *J. Environ. Manag.*, **92**, 407 (2011).
- ⁶ M. Bilal, J. A. Shah, T. Ashfaq, S. M. H. Gardazi, A. A. Tahir *et al.*, *J. Hazard. Mater.*, **263**, 322 (2013).
- ⁷ M. V. Dinu and E. S. Dragan, *React. Funct. Polym.*, **68**, 1346 (2008).
- ⁸ H. Demiral and C. Güngör, *J. Clean Prod.*, **124**, 103 (2016).
- ⁹ T. Todorciuc, L. Bulgariu and V. I. Popa, *Cellulose Chem. Technol.*, **49**, 439 (2015).
- ¹⁰ D. Humelnicu, M. Ignat and F. Doroftei, *Environ. Monit. Assess.*, **187**, 222 (2015).
- ¹¹ E. Guibal, *Sep. Purif. Technol.*, **38**, 43 (2004).

- ¹² A. J. Varma, S. V. Deshpande and J. F. Kenedy, *Carbohydr. Polym.*, **55**, 77 (2004).
- ¹³ W. S. Wan Ngah, L. C. Teong and M. A. K. M. Hanafiah, *Carbohydr. Polym.*, **83**, 1446 (2011).
- ¹⁴ E. S. Dragan, M. V. Dinu and D. Timpu, *Bioresour. Technol.*, **101**, 812 (2010).
- ¹⁵ J. Zeng, H. Chen, X. Yuan, Q. Guo and X. Yu, *Desalin. Water Treat.*, **55**, 1 (2014).
- ¹⁶ C. Xiao, X. Liu, S. Mao, L. Zhang and J. Lu, *Appl. Surf. Sci.*, **394**, 378 (2017).
- ¹⁷ E. S. Dragan and M. V. Dinu, *Res. J. Chem. Environ.*, **17**, 4 (2013).
- ¹⁸ A. I. Cocarta and E. S. Dragan, *Cellulose Chem. Technol.*, **48**, 495 (2014).
- ¹⁹ E. S. Dragan, A. I. Cocarta and M. V. Dinu, *Chem. Eng. J.*, **255**, 659 (2014).
- ²⁰ E. S. Dragan, D. F. Apopei-Loghin and A. I. Cocarta, *ACS Appl. Mater. Interf.*, **6**, 16577 (2014).
- ²¹ W. S. W. Wan Ngah and S. Fatinathan, *J. Environ. Manage.*, **91**, 958 (2010).
- ²² S. Emik, *React. Funct. Polym.*, **75**, 63 (2014).
- ²³ M. Monier, *Int. J. Biol. Macromol.*, **50**, 773 (2012).
- ²⁴ G. Limousin, J. P. Gaudet, L. Charlet, S. Szenknect, V. Barthes *et al.*, *Appl. Geochem.*, **22**, 249 (2007).
- ²⁵ C. H. Giles, D. Smith and A. Huitson, *J. Colloid Interf. Sci.*, **47**, 755 (1974).
- ²⁶ K. Y. Foo and B. H. Hameed, *Chem. Eng. J.*, **156**, 2 (2010).
- ²⁷ S. Vasiliu, I. Bunia, S. Racovita and V. Neagu, *Carbohydr. Polym.*, **85**, 376 (2011).
- ²⁸ D. F. Apopei, M. V. Dinu, A. Trochimczuk and E. S. Dragan, *Ind. Eng. Chem. Res.*, **51**, 10462 (2012).
- ²⁹ K. Hall, L. C. Eagleton, A. Acrivos and T. Vermeulen, *Ind. Eng. Chem. Fund.*, **5**, 212 (1966).
- ³⁰ Y. C. Srivastava, M. M. Swamy, I. D. Mall, B. Prasad and I. M. Mishra, *Colloid. Surf. A*, **272**, 89(2006).
- ³¹ S. Lagergren, *Handlingar*, **24**, 1 (1898).
- ³² Y. S. Ho and G. McKay, *Can. J. Chem. Eng.*, **76**, 822 (1998).
- ³³ E. G. Deze, S. K. Papageorgiou, E. P. Favvas and F. K. Katsaros, *Chem. Eng. J.*, **209**, 537 (2012).
- ³⁴ J. W. J. Weber and J. C. Morris, *J. Sanit. Eng. Div., Am. Soc. Civ. Eng.*, **89**, 31 (1963).
- ³⁵ M. V. Dinu and E. S. Dragan, *Chem. Eng. J.*, **160**, 157 (2010).
- ³⁶ N. B. Milosavljevic, M. D. Ristic, A. A. Peric-Grujic, J. M. Filipovic, S. B. Štrbac *et al.*, *Colloid. Surf. A*, **388**, 59 (2011).
- ³⁷ H. T. Fan, X. T. Sun, Z. G. Zhang and W. X. Li, *J. Chem. Eng. Data*, **59**, 2106 (2014).